

Nanoscale

Accepted Manuscript



This is an *Accepted Manuscript*, which has been through the Royal Society of Chemistry peer review process and has been accepted for publication.

Accepted Manuscripts are published online shortly after acceptance, before technical editing, formatting and proof reading. Using this free service, authors can make their results available to the community, in citable form, before we publish the edited article. We will replace this *Accepted Manuscript* with the edited and formatted *Advance Article* as soon as it is available.

You can find more information about *Accepted Manuscripts* in the [Information for Authors](#).

Please note that technical editing may introduce minor changes to the text and/or graphics, which may alter content. The journal's standard [Terms & Conditions](#) and the [Ethical guidelines](#) still apply. In no event shall the Royal Society of Chemistry be held responsible for any errors or omissions in this *Accepted Manuscript* or any consequences arising from the use of any information it contains.

ARTICLE

Gold nanorods as a theranostic platform for *in vitro* and *in vivo* imaging and photothermal therapy of inflammatory macrophages

Cite this: DOI: 10.1039/x0xx00000x

Received 00th January 2012,
Accepted 00th January 2012

DOI: 10.1039/x0xx00000x

www.rsc.org/

Jinbao Qin ‡^a, Zhiyou Peng ‡^a, Bo Li ‡^b, Kaichuang Ye ^a, Yuxin Zhang ^b, Fukang Yuan ^a, Xinrui Yang ^a, Lijia Huang ^a, Junqing Hu ^{b*}, Xinwu Lu ^{a, c*}

Inflammatory macrophages play pivotal roles in the development of atherosclerosis. Theranostics, a promising approach for local imaging and photothermal therapy of inflammatory macrophages, has drawn increasing attention in biomedical research. In this study, gold nanorods (Au NRs) were **synthesized**, and their *in vitro* photothermal effects on macrophages cell line (Ana-1 cells) under 808 nm near infrared reflection (NIR) were investigated by CCK8 assay, calcein AM/PI staining, flow cytometry, transmission electron microscopy (TEM), silver staining and *in vitro* micro-computed tomography (CT) imaging. These Au NRs were then applied to an apolipoprotein E knockout (Apo E) mouse model to evaluate their effects *in vivo* CT imaging and their effectiveness as for the subsequent photothermal therapy of macrophages in femoral artery restenosis under 808 nm laser irradiation. *In vitro* photothermal ablation treatment using Au NRs exhibited a significant cell-killing efficacy of macrophages, even at relatively low concentrations of Au NRs and low NIR powers. In addition, the *in vivo* results demonstrated that the Au NRs are effective for *in vivo* imaging and photothermal therapy of inflammatory macrophages in femoral artery restenosis. This study shows that Au nanorods are a promising theranostic platform for the diagnosis and photothermal therapy of inflammatory-associated diseases.

1. Introduction

Inflammatory macrophages play pivotal roles in the progress of atherosclerosis (AS) because macrophages can release inflammatory factors and chemokines, which may accelerate the damage to normal vessels and promote the neointimal proliferation or restenosis after interventional therapies.^{1, 2} Recent studies showed that a high macrophage burden is one of the primary factors contributing to plaque formation and restenosis, which may cause serious complications or death.³

^a Department of Vascular Surgery, Shanghai Ninth People's Hospital, Shanghai JiaoTong University School of Medicine, Shanghai 200011, China

^b State Key Laboratory for Modification of Chemical Fibers and Polymer Materials, College of Materials Science and Engineering, Donghua University, Shanghai 201620, China

^c Vascular Center of Shanghai JiaoTong University, Shanghai 200011, China

*To whom correspondence should be addressed. E-mail addresses: luxinwu@shsmu.edu.cn (X. Lu) and hu.junqing@dhu.edu.cn (J. Hu).

† Electronic supplementary information (ESI) available: Figures.

‡ These authors contributed equally.

Thus, developing new strategies for imaging the extent and invasion depth of macrophages in the atherosclerotic regions and ablating them will be of great value in predicting, prevention, and treatment of AS.

Recently, photothermal therapy (PTT) originated from photothermal agents (such as, noble metal nanostructures, polypyrrole, semiconductor nanostructures, carbon-based materials, and **hybrid nanoparticles**) has attracted increasing attention in treating many diseases,^{4,7} because of its noninvasive feature and minimal side effects compared with traditional methods, including surgery and chemotherapy.⁸⁻¹¹ Among the photothermal agents, Au nanorods (NRs) are well-known contrast agents for computed tomography (CT) and PTT,^{12, 13} because of their large X-ray attenuation coefficient, strong and broad absorption band in the near-infrared region (NIR, 600-900 nm), high photothermal conversion efficiency, excellent biocompatibility and stability during laser irradiation. Therefore, Au NRs are expected to be an ideal theranostic platform for enhanced *in vivo* CT imaging and the subsequent PTT.

Inflammatory macrophages ablation has shown great potential in treating atherosclerotic diseases,^{14, 15} and recent studies using Au nanoparticles and other agents have demonstrated effective effects on macrophage ablation in animal models.¹⁶ However,

studies on the use of Au NRs for *in vitro* and *in vivo* micro-CT imaging and PTT of macrophages in the femoral artery restenosis are limited. In this study, gold nanorods (Au NRs) were synthesized and characterized by TEM and UV-vis-NIR. *In vitro* CCK8 assay of cytotoxicity and flow cytometry analysis of macrophage cell (Ana-1 cells) cycles and apoptosis show that the Au NRs are non-cytotoxic and have good biocompatibility at the given concentration (20 $\mu\text{g}/\text{mL}$). TEM and silver staining further confirm that the macrophages can phagocytize Au NRs and can be imaged by Micro-CT. Importantly, after under 808 nm laser irradiation (0-2 W/cm^2 , 5 min), the Calcein AM/PI staining results demonstrates the formed Au NRs exhibiting excellent photothermal conversion effects on Ana-1 cells. Subsequently, these Au NRs were applied to an apolipoprotein E (Apo E) knockout mouse model for femoral artery restenosis to evaluate its *in vivo* CT imaging and subsequent photothermal therapy of inflammatory macrophages in the restenosis under 808nm laser irradiation. As far as we know, this research is the first one that reports the Au NRs can be used as a theranostic platform for dual imaging and photothermal therapy of inflammatory macrophages, which will pave the way for further PTT of other inflammatory diseases.

2. Materials and methods

2.1 Materials

Gold(III) chloride, ascorbic acid, silver nitrate, and hexadecyltrimethyl ammonium bromide (CTAB) were purchased from Aladdin and used as received without further purification. A mouse macrophage cell line, Ana-1, was purchased from Shanghai Cell Bank, the Chinese Academy of Sciences (Shanghai, China). Fetal bovine serum, Dulbecco's modified Eagle's medium (DMEM), penicillin, and streptomycin were obtained from GIBCO Company and SIGMA Company. All other chemicals were from Sinopharm Chemical Reagent Co., Ltd. (Shanghai, China) and used as received. Water used in all experiments was purified using a Milli-Q Plus 185 water purification system (Millipore, Bedford, MA) with resistivity higher than 18 $\text{M}\Omega\text{ cm}$.

2.2 Synthesis and Characterization of Gold Nanorods

Au NRs were synthesized via a modified method from literature.^{17, 18} Briefly, a seed solution was prepared by reducing gold(III) chloride (25 mL, 0.05 M) in hexadecyltrimethyl ammonium bromide (CTAB, 4.7 mL, 0.1 M) by adding freshly prepared sodium borohydride (0.3 mL, 0.01 M) under vigorous stirring. An aliquot of seed solution (0.24 mL) was added to a growth solution containing that contains CTAB (100 mL, 0.1 M), gold(III) chloride (1.0 mL, 0.05 M), hydrochloric acid (2 mL, 1 M), 0.8 mL of ascorbic acid and silver nitrate (1.2 mL, 0.01 M). The glass beaker was placed in a water bath maintained at 27 °C for 6 h to complete the synthesis. Aliquots (50 mL) of the synthesized rods were centrifuged at 8000 rpm for 10 min to obtain pellets of Au NRs at the bottom of the tube. The supernatant was decanted, the pellet was re-dispersed into deionized water, and then centrifuged for another time. Then, 1 mL of cystamine dihydrochloride (30 mM) was added. The solution was kept at 50°C under constant sonication for 3 h and then centrifuged twice at 7000 rpm for 10 min to remove excess CTAB (CTAB is known to be cytotoxic) and cystamine dihydrochloride.

The morphologies, and sizes of the synthesized Au NRs were analyzed using high-resolution TEM (HR-TEM, JEM-2100 LAB6, JEOL Ltd., Japan). TEM was performed on a Hitachi H-800L0 TEM instrument at an accelerating voltage of 200 kV. Approximately 3 mL drops of Au NRs solutions (centrifuged

and resuspended in deionized water) were dried on carbon-coated copper grids for 0.5 h. TEM micrographs of at least eight different regions of the grid were obtained. In addition, the UV-visible absorption spectra of the samples were determined by a spectrometer (Optizen 2120UV, Mecasys, Korea). **Zeta potential measurements were carried out with the Zetasizer Nano Z (Malvern, Britain).** The photothermal conversion performances of Au NRs were measured using our previously reported method.^{19, 20} To measure the photothermal effect of Au NRs, 0.3 mL aqueous dispersion with different concentrations (0 – 40 ppm) were irradiated by a 808 nm laser (~ 0.8 W for a spot size of ~ 0.40 cm^2). A thermocouple with an accuracy of ± 0.1 °C was inserted into the aqueous dispersion at such a position that the direct irradiation of the laser on the probe was avoided. The temperature was recorded by an online type thermocouple thermometer (DT-8891E Shenzhen Everbest Machinery Industry Co., Ltd., China) every 5 s.

2.3 Cell culture and characterization

Ana-1 cells, a mouse macrophage cell line, were obtained from Shanghai Cell Bank, the Chinese Academy of Sciences (Shanghai, China). Macrophages were cultured in RPMI 1640 medium (Gibco, Gaithersburg, MD) supplemented with 10% fetal bovine serum (FBS, Gibco, USA) and 1% streptomycin/penicillin Sigma (St. Louis, MO) at 37 °C under 5% CO_2 .

To analyze the specific protein markers of macrophages, Ana-1 cells were investigated by immunofluorescence staining and flow cytometry in accordance with our previous report.²¹ Briefly, Ana-1 cells were plated at a density of 1×10^6 cells per well and cultured in six-well plates. After 24h incubation, the cells were fixed with 4% paraformaldehyde (PFA) for 20 min. After washing in phosphate-buffered saline solution (PBS), the cells were permeabilized in 0.3% Triton-X100, and blocked with 10% goat serum for 30 min at 37 °C. The macrophages were then incubated with macrophage specific proteins F4/80 (rat monoclonal, 1:500, Abcam, UK), Iba-1 (rat monoclonal, 1:500, Abcam, UK) and MAC-3 (rat monoclonal, 1:500, BD, California, USA) for 24 h at 4 °C. Cells incubated with PBS served as the negative control. After PBS washing, the secondary antibody Alexa Fluor® 555 and Alexa Fluor® 488 (goat anti-rat, 1:500, Invitrogen, USA) was applied and incubated for 45 min at 37 °C in the dark. After washing in PBS, the cells were stained with 4', 6-diamidino-2-phenylindole (DAPI) (1:500, DAKO, USA). The macrophages were then analyzed under a fluorescence microscope (Olympus, Japan).

For flow cytometry analysis, 1×10^6 Ana-1 cells were collected and incubated with phycoerythrin (PE)-conjugated macrophage surface antibodies F4/80 (Abcam, UK) and CD11b (BD, USA) for 45 min in the dark on the ice. Isotype antibodies were used as control. After washing in PBS, cells were analyzed using a flow cytometer (Beckman Coulter, Fullerton, CA).

2.4 Cellular uptake of Au NRs and photothermal treatment

A CCK8 cell proliferation assay (Dojindo Laboratories, Kumamoto, Japan) was used to evaluate the viability of the macrophages treated with different concentrations of Au NRs as we previously reported.²² Briefly, 2.0×10^4 Ana-1 cells/well were seeded in triplicate into a 96-microwell plate and incubated for 24 h at 37 °C. The Ana-1 cells were then treated with various concentrations of Au NRs (0, 5, 10, 20 and 40 $\mu\text{g}/\text{mL}$, respectively) and incubated for 24 h at 37 °C in a humid 5% CO_2 incubator. After washing with PBS, 10 μL of CCK8 reagent (in 100 μL PBS) was added and incubated for 2 h. The

assays were performed in accordance with the manufacturer's instructions. For each concentration of Au NRs, the mean and standard deviation for the quadruplicate wells were reported. One-way ANOVA was used to evaluate the differences of the viability of cells treated with Au NRs with different concentrations and the control cells treated with PBS.

For the NIR laser irradiation experiment, Ana-1 cells were pre-cultured in 96-well cell culture plates (2.0×10^4 per well) for 24 h, then Au NRs (20 $\mu\text{g}/\text{mL}$) were added, and the cells were irradiated by an 808 nm laser for 5 min at three different powers (0.5, 1 and 2 W/cm^2) at a distance of 7 cm. After 24 h incubation, standard CCK8 assay was performed to analyze the cell viabilities relative to the control untreated cells (incubated with PBS), the experiments were performed in triplicate.

After laser irradiation, the Ana-1 cells were also stained with calcein acetoxymethyl ester (calcein AM, 1 μM , Molecular Probes, USA) and propidium iodide (PI) to distinguish the live from dead cells through a fluorescence microscope (Olympus, Japan). Fluorescence images of more than three different areas in each sample were obtained. After laser irradiation, the cells treated with Au NRs (20 $\mu\text{g}/\text{mL}$) without or with PTT were harvested, centrifuged, and resuspended in PBS at 1×10^6 cells per mL to analyze the macrophage cycles and apoptosis. The cell suspensions were counterstained with PI and Annexin V (eBioscience, San Diego, USA). The cell cycle (G0-G1, G2-M, S phases, and apoptosis) were quantified using the Cell Quest software (FACS Calibur, Becton Dickinson, USA).

2.5 Intracellular TEM

To evaluate the photothermal effects of Au NRs on the organelle of macrophages, TEM imaging was performed according to our previous report.²³ Briefly, 3×10^6 Ana-1 cells were treated with Au NRs (20 $\mu\text{g}/\text{mL}$) for 24 h at 37 °C, untreated cells were also prepared. After irradiation by the 808 nm laser, the cells were trypsinized, centrifuged, and fixed with 2.5% glutaraldehyde for 12 h at 4 °C and post-fixed with 1% OsO₄ in 0.2 M phosphate buffer (pH 7.2) for 2 h at 4 °C. After washing for three times with PBS, the cells were dehydrated, infiltrated with propylene oxide and embedded with Epon 812 (Shell Chemical, UK) for polymerization. Furthermore, the embedded cells were cut into a thickness of 75 nm using a Reichert Ultramicrotome and mounted onto 200 mesh copper grids. After counterstaining with uranyl acetate and lead citrate for 5 min, all of the samples were observed using TEM (H600 TEM, Hitachi, Japan) at an acceleration voltage of 60 kV.

2.6 Silver staining and micro-CT imaging of macrophages

To evaluate the cellular uptake of Au NRs, Ana-1 cells treated with Au NRs were verified by silver staining and *in vitro* micro-CT imaging. Briefly, for silver staining, Ana-1 cells (2×10^6 /well) were cultured and incubated with different concentrations of Au NRs (10, 20 and 40 $\mu\text{g}/\text{mL}$) for 24 h at 37 °C. Ana-1 cells incubated with PBS served as a negative control. After washing, silver staining was performed according to the manufacturer's instruction.

For *in vitro* micro-CT imaging, 5.0×10^6 Ana-1 cells incubated with different concentrations of Au NRs (10, 20 and 40 $\mu\text{g}/\text{mL}$) were trypsinized, resuspended with 100 μL PBS in a 0.5 mL Eppendorf tube, and then scanned using a micro-CT imaging system (eXplore Locus, GE Healthcare, London, Ontario, Canada). CT values were analyzed, each experiment was performed in triplicate.

2.7 Animal model and in vivo thermal therapy

Animal experiments and animal care were conducted in accordance with the protocols approved by the Animal Experiment and Care Committee of Shanghai JiaoTong

University School of Medicine. Macrophage-rich atherosclerotic lesions were created in the right femoral arteries of ApoE mice, as previously described.²⁴ In summary, 8 month-old male Apo E knockout (C57BL/6 background, n=16) mice fed with a Western-type diet (containing 21% fat, 0.15% cholesterol) were obtained from Shanghai Research Center for Model Organisms (Shanghai, China). The mice were anesthetized with an intraperitoneal injection of 40 mg/kg pentobarbital sodium. The right femoral artery was dissected and sheathed with a polyethylene cuff placement (Milaty, Zhangjiagang, China) to induce atherosclerotic-like restenosis formation as described previously (23). The left femoral artery was also isolated from surrounding tissues (sham-group, n = 8), but a cuff was not placed. Then the skin was sutured with 5/0 silk, and the animals were recovered on a warming box.

Fourteen days after surgery, the mice of each group were intravenously injected with 100 μL Au NRs (0.4 μmol Au per g body weight) through the tail vein. After that, the mice were scanned by a GE Healthcare micro-CT with an imaging system (eXplore Locus, USA) with a tube voltage of 80 kV, an electrical current of 450 μA , and a slice thickness of 45 μm .

For photothermal treatment, after micro-CT imaging, the mice of each group were immediately irradiated with continuous NIR laser in regions of femoral artery restenosis for 10 min at the power density of 2 W/cm^2 . The local temperature of femoral artery restenosis regions under the laser irradiation was measured using an infrared (IR) imager (GX-300; Shanghai Infratec Electronics Co., Shanghai, China).

2.8 Bio-distribution of Au NRs and histological staining

To study the bio-distribution of Au NRs, the mice (n=6) were anesthetized with pentobarbital sodium after PTT. Subsequently, the heart, lung, stomach, spleen, liver, intestines, kidney, testicle, blood, and brain were collected and weighed. The samples were cut into 1–2 mm^3 pieces and incubated in aqua regia solution for 4 h. Au concentrations were quantified by inductively coupled plasma mass spectrometry (a Leeman Prodigy ICP-AES system, Hudson, NH03051, USA).

For histological staining, the mice were anesthetized and perfusion-fixed after PTT. The femoral arteries, heart, lungs, liver, spleens, kidneys, and intestines were extracted and immediately fixed in 4% PFA. The organs were then dehydrated and embedded in paraffin. The organs were cut into 5 μm sections using a conventional microtome.

For immunohistochemical staining, the femoral arteries were dewaxed, antigen retrieval and incubated with primary macrophage specific antibody CD68 (rat monoclonal, 1:200) for 24 h at 4 °C. As a negative control, the primary antibody was replaced with PBS. After washing with PBS, the arteries were incubated with secondary biotinylated antibodies (goat anti-rat, 1:200) for 1 h at 37 °C. After washing thrice, the arteries were finally incubated with ABC complex reagent and 3, 3'-diaminobenzidine (DAB). After washing and then staining with hematoxylin, the samples were viewed under a light microscope (Nikon, Tokyo, Japan).

2.9 Statistics

All of the quantitative data were expressed in the form of means \pm S.D. T test is applied for comparison between two groups by SPSS 18.0 software. For the comparison among multiple groups, one-way ANOVA was used, and when there's a difference LSD's tests were followed. 0.05 was considered as a significance level and the data were labeled with (*) for $p < 0.05$, (#) for $p < 0.01$, and (&) for $p < 0.001$ respectively.

3. Results and discussion

3.1 Au NRs synthesis and characterization

In the work presented here, gold nanorods (Au NRs) were synthesized and characterized by TEM and UV-vis-NIR. A TEM image in Fig 1a shows good monodispersity of the resulting Au NRs with a mean size of $\sim 68 \text{ nm} \times 15 \text{ nm}$. **TEM image revealed that the Au NRs showed a mean size of $\sim 60 \text{ nm} \times 15 \text{ nm}$ (Fig S1). For very small gold nanomaterials ($< 4 \text{ nm}$), their chemical reactivity becomes important, and oxidative damage to cells is possible,²⁵⁻²⁷ while larger nanomaterials ($> 100 \text{ nm}$) could be removed by the reticuloendothelial system, primarily by the liver and spleen, and smaller particles by the renal system,^{28,29} we thus believe our as-prepared Au NRs are suitable for photothermal therapy.** As shown in Fig 1b, the UV-vis spectrum of Au NRs showed a sharp and strong absorption centered at $\sim 840 \text{ nm}$. Owing to their strong NIR absorption

feature and the location of maximum absorption wavelength, the Au NRs exhibit their potential in photothermal ablation therapy of macrophages using a 808 nm wavelength laser. Under continuous irradiation of the laser at 0.29 W, the temperature elevation of aqueous dispersions containing Au NRs at different concentrations (0–20 ppm) was measured, as shown in the Fig 1c. The control experiment demonstrates that the temperature of pure water (without Au NRs) is only increased by less than 3.0°C (from the room temperature, 22°C) in 7 min. With the addition of the Au NRs (i.e., 5, 10 and 20 ppm), the temperature of the aqueous dispersion increased by $6.0\text{--}19.5^\circ\text{C}$ after 7 min of irradiation, which indicates that the Au NRs can rapidly and efficiently convert the 808 nm wavelength laser energy into heat energy as a result of the strong photo-absorption at 808 nm.

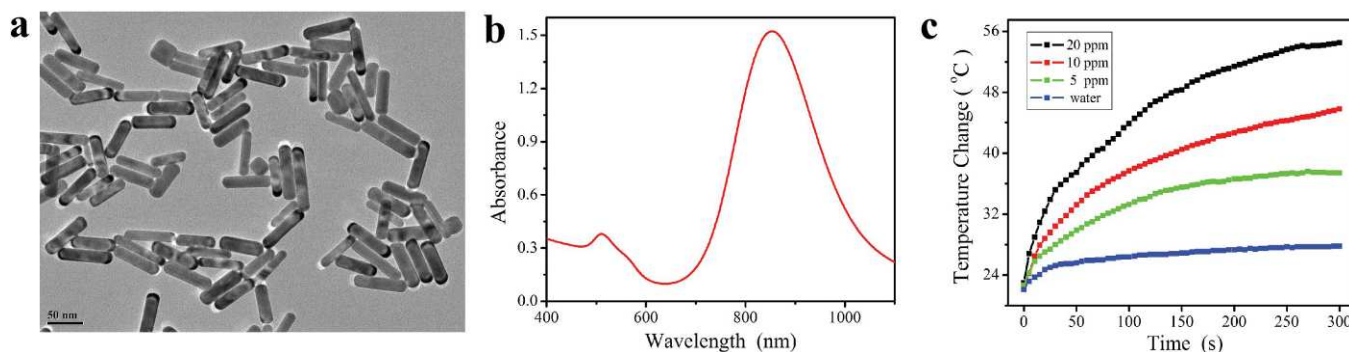


Fig. 1 Preparation and characterization of the Au NRs. (a) TEM image of the Au NRs. (b) UV-vis-NIR absorbance spectrum of the Au NRs' solution. (c) Heating curves of pure water and different concentrations of the Au NRs (5, 10, and 20 ppm) under the 808 nm laser irradiation at a power density of 2 W/cm^2 .

3.2 Cellular uptake of Au NRs and photothermal treatment

Ana-1 cells, a mouse macrophage cell line, were used in our study. To analyze the specific protein markers of macrophages, Ana-1 cells were investigated by immunofluorescence staining and flow cytometry. After 48 h of culturing, the round-shaped Ana-1 cells proliferated rapidly and were passaged every other day. Immunofluorescent staining demonstrated that these Ana-1 cells were positive for macrophage-specific proteins F4/80 (red), Iba-1 (green), and MAC-3 (red) and the nuclei were stained with DAPI (blue, Fig. S2a). In addition, flow cytometry analysis further revealed that the Ana-1 cells were strongly positive for the macrophages surface antigens F4/80 ($98.7\% \pm 0.37\%$, Fig. S2b) and CD11b ($98.1\% \pm 0.23\%$, Fig. S1c) compared with the control groups ($0.3\% \pm 0.02\%$, Fig. S1d).

The zeta potential of gold nanorods changed from $+30.5 \pm 8.2 \text{ mV}$ to $+2.5 \pm 5.1 \text{ mV}$ after modification by cystamine dihydrochloride, indicating the removal of CTAB from the surface of Au NRs. Despite the excess CTAB was removed by centrifugation, some CTAB may still adsorb on Au nanorods. Prior to using the formed Au NRs, the *in vitro* cytotoxicity and apoptosis of the Au NRs to macrophages should be evaluated. In our study, we examined the viability of the concentration-dependent effects of the Au NRs on the Ana-1 cells using CCK8 assay. Fig 2a showed that Ana-1 cells do not display any appreciable morphological changes at the Au NRs concentration up to $20 \mu\text{g/mL}$ when compared with the control cells treated with PBS. When the Au NRs concentration reached $40 \mu\text{g/mL}$, the viability of the Ana-1 was slightly affected. The results clearly suggest the good biocompatibility **and lower toxicity** of the Au NRs in a concentration range of

$0\text{--}20 \mu\text{g/mL}$. Compared with other reports, our Au NRs exhibited a considerably lower cytotoxicity, even at a high concentration of $40 \mu\text{g/mL}$.²⁵

These nontoxic surface-modified Au NRs were then investigated for their PTT efficiency with macrophages. A NIR-coherent diode laser (808 nm) was used to irradiate each well for 5 min with a different laser power density ($0.5, 1.0$ and 2.0 W/cm^2). According to literature, the NIR light ($650\text{--}950 \text{ nm}$) is generally accepted, not only can it penetrate the deep tissues, it is also relatively lowly absorbed by hemoglobin in blood and causes less damage to other normal tissues.²⁶ The Ana-1 cells treated with the Au NRs ($20 \mu\text{g/mL}$) exhibited power-dependent cytotoxicity (Fig. 2b), suggesting an intrinsic cytotoxicity that could lead to systemic side effects. By contrast, the Ana-1 cells incubated with Au NRs without irradiation were not affected. Consequently, our *in vitro* photothermal therapy of Ana-1 cells using the Au NRs exhibited a significant cell-killing efficacy, even with a relatively lower concentration of the Au NRs ($20 \mu\text{g/mL}$) and a lower NIR power (2.0 W/cm^2) than those in previous reports.^{12, 27}

After the NIR irradiation, calcein AM/PI staining was conducted to classify the live and dead cells. As shown in Fig 2c, the untreated control cells showed green nuclei and uniform chromatin, which imply that they were live and healthy cells. Similarly, most of the Ana-1 cells incubated with the same Au NRs ($20 \mu\text{g/mL}$) with increasing the NIR laser powers from 0.5 to 2.0 W/cm^2 showed color change from orange to red. Thus, they were suffering from apoptosis, in which some cells were in the late stages of apoptosis (Fig. 2c). Statistical analysis of the

relative cell viabilities further demonstrated that with the increase of the NIR laser power from 0.5 W/cm² to 2.0 W/cm², more cells incubated with Au NRs were killed by the laser ablation (Fig. S3). By contrast, these Ana-1 cells without Au NRs treatment were unaffected even after a higher laser irradiation (Fig. S3), which were consistent with CCK8 results. The results suggest that the Ana-1 cells internalized the Au NRs, which adsorbed and transformed the NIR laser power into heat. As temperatures increase to more than 40°C, irreversible damage occurs in the organelles.²⁸ These result in the denaturation of the proteins and the dissolution of nucleus karyotheca, ultimately triggering cell death.

To investigate the photothermal effect of the Au NRs on Ana-1 apoptosis and cell cycles, the treated cells were incubated in Annexin V/PI and analyzed by a flow cytometry after the laser irradiation. The percentages of apoptosis and cell phase distribution in untreated Ana-1 and treated Ana-1 cells without or with PTT were 3.62% ± 0.58%, 4.35% ± 0.63% and 19.91% ± 2.87%, respectively, with statistically significant differences between the Au NRs groups and the control groups ($P < 0.05$, Fig. 3a). The representative flow cytometric peaks and the percentage of the cell cycle in the G0/G1, S, and G2/M phases are presented in Fig 3b. The cell cycle phases of the Ana-1 cells incubated with the Au NRs and PTT showed

significant differences compared with those of the untreated negative control cells and the Au NRs treated without PTT groups (data not shown). These results further demonstrate that the Au NRs are noncytotoxic at the given concentration and exhibit excellent PTT effects of macrophages.

3.3 Intracellular TEM

In Fig 4b and e, after incubation with the Au NRs, a large amount of electron-staining particles were found in the intracellular region (as indicated by the red arrow), mostly in the endosomes/lysosomes. After the NIR irradiation, the TEM image (Fig. 4c and f) showed that some nucleus karyotheca were dissolved and broken, and the nucleolus and the endoplasmic reticulum disappeared. In addition, the Au NRs were internalized in the Ana-1 cells cytoplasm (as indicated by the red arrow). By contrast, no black clusters were observed in the untreated control Ana-1 cells and the cellular structures were not damaged (Fig. 4a and d), which are consistent with the results of the calcein AM/PI staining. The internalization of the Au NRs may occur through two different mechanisms: phagocytosis and receptor-mediated endocytosis via cell walls.^{29, 30}

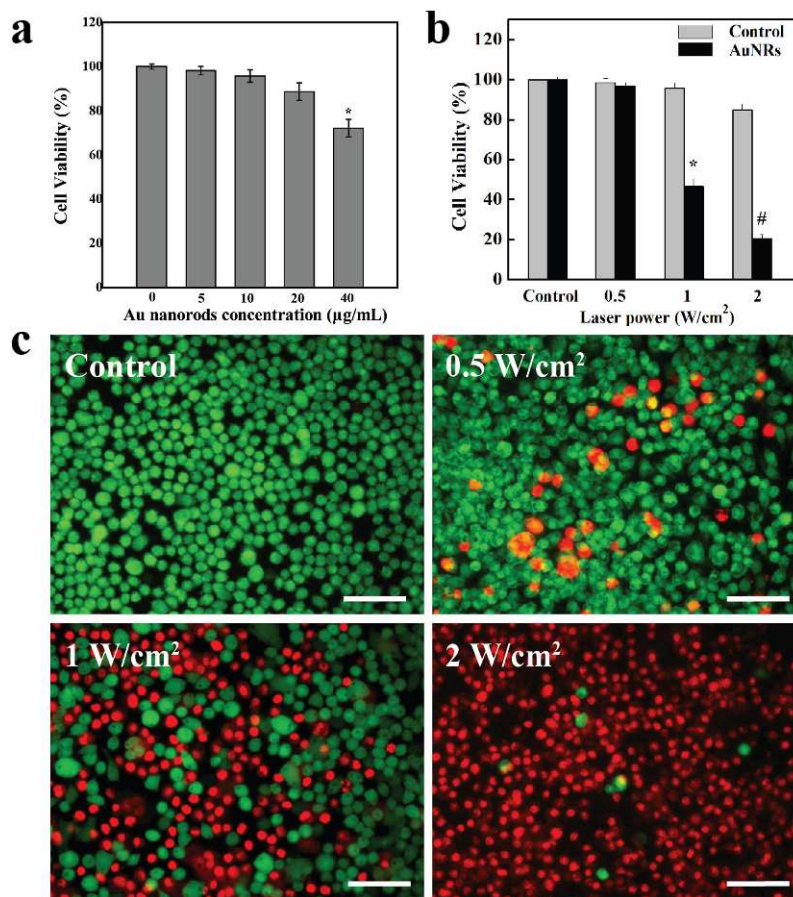


Fig. 2 Cytotoxicity of Au NRs and PTT. (a) *In vitro* cell viability of Ana-1 cells treated with or without various concentrations of the Au NRs for 24 h. (b) Cell viability of Ana-1 cells treated with or without the Au NRs (20 µg/mL) after the NIR laser irradiation with different power densities (0, 0.5, 1 and 2 W/cm²). (c) Live cells and dead cells were stained with calcein AM (green) and PI (red), after incubation of Ana-1 cells with or without the Au NRs (20 µg/mL) and being exposed to the 808 nm laser at different power densities (0.5, 1 and 2 W/cm²). Scale bar: 100 µm.

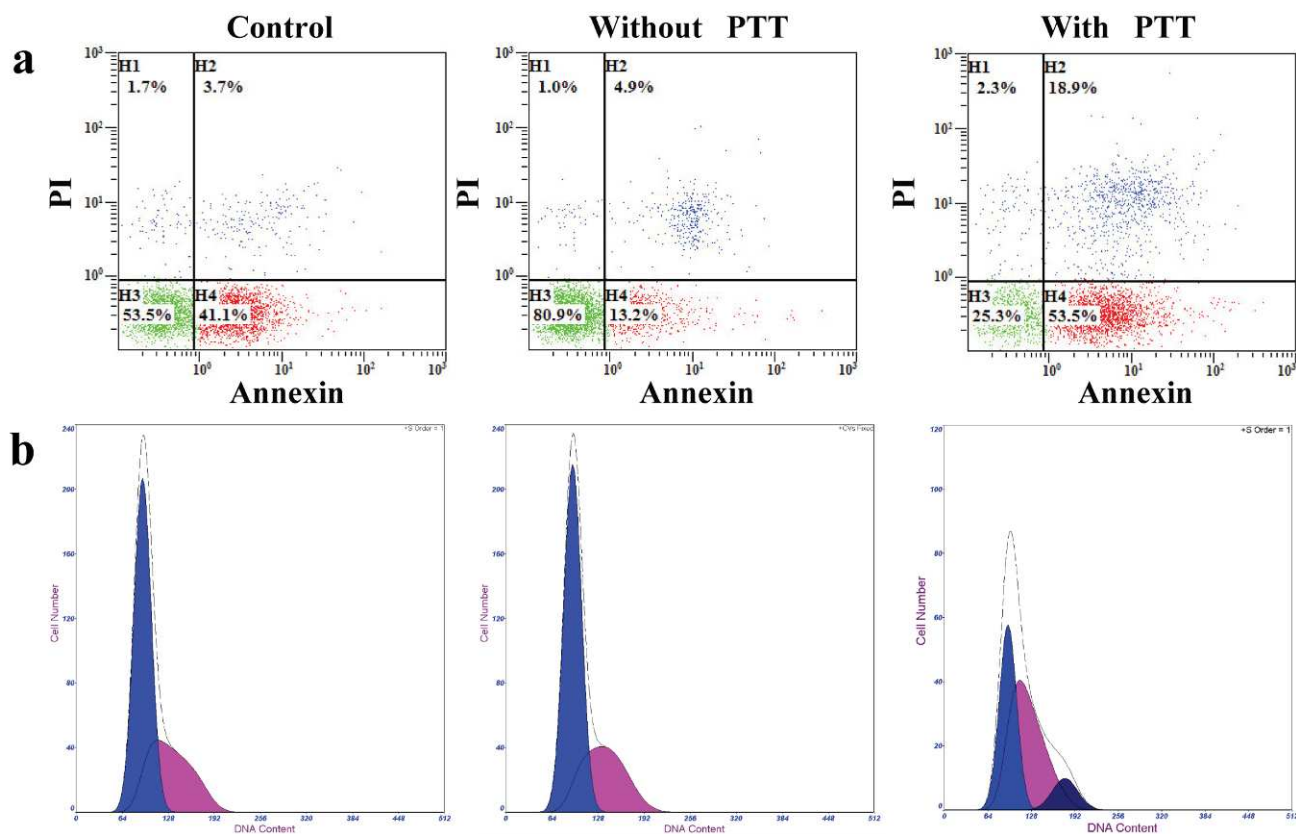


Fig. 3 Flow cytometric analysis of cell cycles and apoptosis of Ana-1 cells treated without Au NRs and treated with Au NRs with or without PTT ($n=4$).

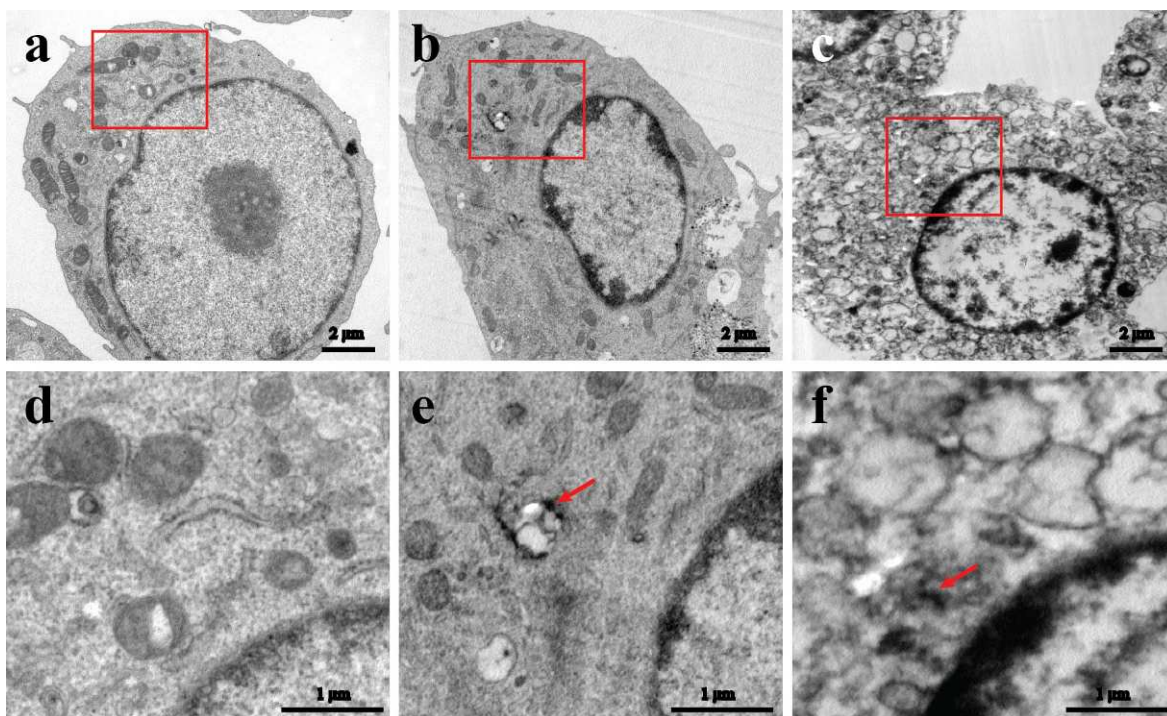


Fig. 4 TEM images of Au NRs-loaded cells after laser irradiation. (a) TEM images of control Ana-1 cells, no black clusters were observed in the cytoplasm. (b) TEM images of Ana-1 cells incubated with Au NRs (20 $\mu\text{g}/\text{mL}$) for 24 h, Au NRs are mainly located in the endosomes/lysosomes (indicated by the red arrow). (c) After NIR irradiation, the TEM image shows that some nucleus karyotheca were dissolved and broken, and the nucleolus and the endoplasmic reticulum disappeared, the Au NRs are internalized in the Ana-1 cells cytoplasm (indicated by the red arrow). Scale bar measures 2 μm . (d) High-magnification TEM images of (a). (e) High-magnification TEM images of (b). (f) High-magnification TEM images of (c). Scale bar measures 1 μm .

3.4 Silver staining and micro-CT imaging of macrophages

To evaluate the cellular uptake of Au NRs, the Ana-1 cells uptake of the Au NRs was subjected to silver staining and *in vitro* micro-CT imaging. As shown in Fig 5, accumulated black spots were observed in the cytoplasm of the Ana-1 cells treated with different concentrations of the Au NRs, i.e., 10 $\mu\text{g}/\text{mL}$ (b), 20 $\mu\text{g}/\text{mL}$ (c) and 40 $\mu\text{g}/\text{mL}$ (d), for 24 h after silver staining. With an increase of the Au NRs concentration, the color of the spots becomes darker, which demonstrates the increase of the cellular phagocytosis of these Au NRs. By contrast, no black spots were observed in the Ana-1 cells treated with PBS (Fig. 5a).

The Ana-1 cells treated with different Au NRs concentrations (10, 20 and 40 $\mu\text{g}/\text{mL}$) for 24 h were also subjected to *in vitro* CT imaging. Fig 5e shows that the macrophage pellets incubated with the Au NRs appear bright, whereas the negative control pellets treated with PBS are indistinguishable. With an increase in the concentration of the Au NRs, the color of the CT images becomes brighter. After quantitative analysis of the CT values of the Ana-1 cells with the Au NRs (Fig. 5f), it is found that the CT value of the Ana-1 cells treated with the Au NRs (40 $\mu\text{g}/\text{mL}$) was significantly higher than that of the cells

incubated at 10 $\mu\text{g}/\text{mL}$ ($p < 0.01$) and 20 $\mu\text{g}/\text{mL}$ ($p < 0.05$) and that of the negative control cells ($p < 0.001$). The higher CT values of the Ana-1 cells at a higher concentration of the Au NRs may be due to the cellular uptake of more Au NRs, which is in consistent with the results of silver staining.

3.5 *In vivo* thermal therapy

We obtained 3D CT images of Apo E mice model of the femoral artery restenosis (which is a widely accepted model for atherosclerotic restenosis²⁴) before and after intravenous injection of the Au NRs. **All the Apo E mice were alive, and no tumor formed in the mice.** Although distinguishing the femoral artery from the surrounding normal tissues in the pre-injected image (Fig. 6b) is difficult, the femoral artery restenosis regions showed slightly enhanced intensity with higher CT values (data not shown) after the injection of the Au NRs (Fig. 6a), as shown in the cuff placement framed by the rectangle in Fig 6b. We presumed that an inflammatory reaction occurred in the right femoral artery after the cuff placement, as suggested by histological examination in Fig 6g and 6h.

Although cancer cells *in vivo* can be efficiently killed through PTT,^{31, 32} rare reports have demonstrated the efficacy of PTT against macrophages.

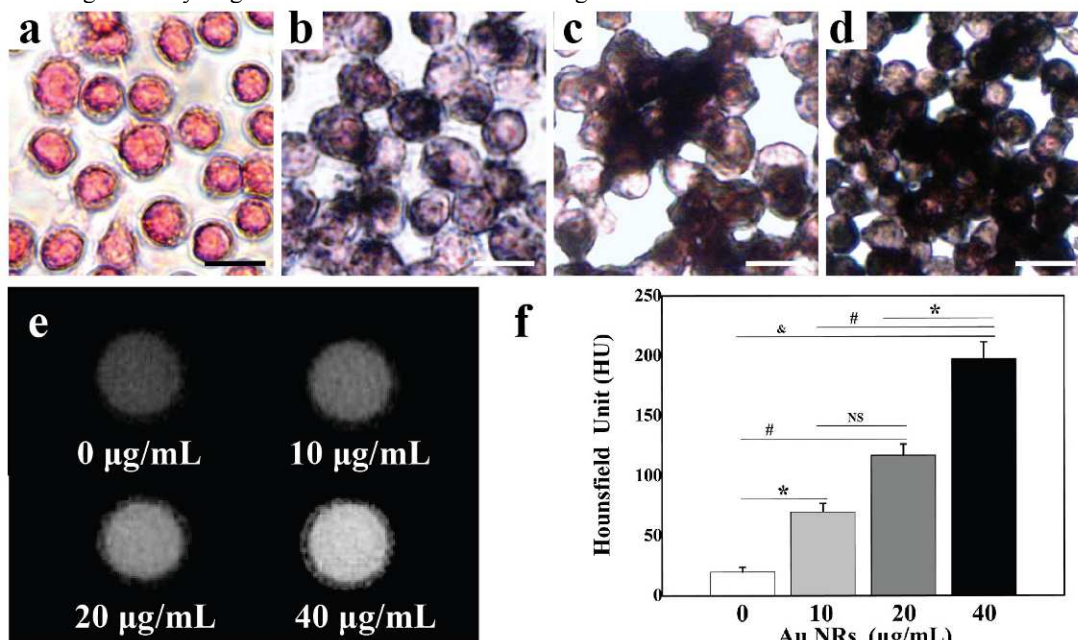


Fig. 5 Representative images of the Ana-1 cells after silver staining and micro-CT imaging. (a) Negative control cells treated without the Au NRs, and the cells incubated with different concentrations of the Au NRs (10 $\mu\text{g}/\text{mL}$ (b), 20 $\mu\text{g}/\text{mL}$ (c) and 40 $\mu\text{g}/\text{mL}$ (d), for 24h. All scale bars: 100 μm . Representative transverse micro-CT images (e) and CT values (f) of the Ana-1 cell suspensions incubated with different concentrations of the Au NRs for 24 h ($n = 3$).

This paper presents the Au NRs-induced PTT against macrophages using a 808 nm laser ($2 \text{ W}/\text{cm}^2$). During the laser treatment, full-body IR thermal images were captured using an IR camera, by which IR thermal images with high contrast could be achieved (Fig. 6c). We can clearly see that the region 11 framed area, which was injected with the Au NRs' solution, generates more significant temperature increases under the laser irradiation (Fig. 6c); by contrast, very little temperature change was detected in region 12 framed area in the control (Fig. 6d). The temperature of the irradiated area was also recorded as a function of the irradiation time (Fig. 6e). For the mice injected with the PBS, the surface temperature of the femoral artery restenosis regions increased by less than 2°C , and remained below 31°C in the entire irradiation process. However, in the

case of the Au NRs-injected mice (Fig. 6c), the surface temperature of the femoral artery restenosis regions increased rapidly and reached up to 50.5°C , **which is due to the good photothermal effect of Au NRs and the enhanced photothermal performance from Au NR aggregation in colloidal solution.**³³ as shown in Fig 6e. These results showed a rapid elevation of temperature of the *in vivo* femoral artery restenosis, which suggests that the Au NRs have an excellent photothermal effect *in vivo*.

3.6 Bio-distribution of Au NRs and histological staining

To evaluate the photothermal ablation of the macrophages *in vivo*, histological examination of the femoral arteries was performed by means of microscopic imaging (Fig. 6f and 6g). Significant macrophage damage was noticed only in the

femoral artery restenosis regions with injected Au NRs, but not in the control group. Those injected with the Au NRs show a decrease in the number of macrophages in comparison with the control injected with the PBS (Fig. 6h). In addition, the corresponding histological staining further confirms that the intima media of the Au NRs groups was significantly thinner than that of the control groups (data not shown).

These results suggest that the macrophages can be efficiently destroyed *in vivo* by high temperature (49.5 ± 1.7 °C) because of the excellent photothermal effect of the Au NRs. The ablation effects of the PTT are dependent on the temperature of targeted regions and time. At 46 °C, irreversible cellular apoptosis was observed after 60 min, but a time of 4-6 min is sufficient at 50-52 °C.^{34,35} Therefore, the synthesized Au NRs with excellent photothermal effects can be used as theranostic agents for *in vivo* imaging and PTT of inflammatory diseases.

Understanding the bio-distribution of the Au NRs is crucial for their use as a theranostic platform for their *in vivo* PTT of macrophages. The bio-distribution of the Au NRs in the major organs (heart, lung, liver, spleen, stomach, intestines, kidney, testicle, and blood) after the PTT was quantified by ICP-AES (Fig. 7a). Large amounts of Au element were found in the spleen and liver, which are known as the reticuloendothelial system (RES).^{36,37} **This result indicates that aside from the accumulation within macrophages, the Au NRs can be cleared mainly through the renal/urinary route and RES.**^{38,39} By contrast, no obvious Au element was found in the untreated group. Future efforts for reducing the capture by RES and detailed pharmacokinetic studies of the Au NRs are needed for better understanding. Overall, our bio-distribution studies show that the developed Au NRs can be uptaken by these macrophages via different administration routes, thereby allowing effective PTT of the macrophages.

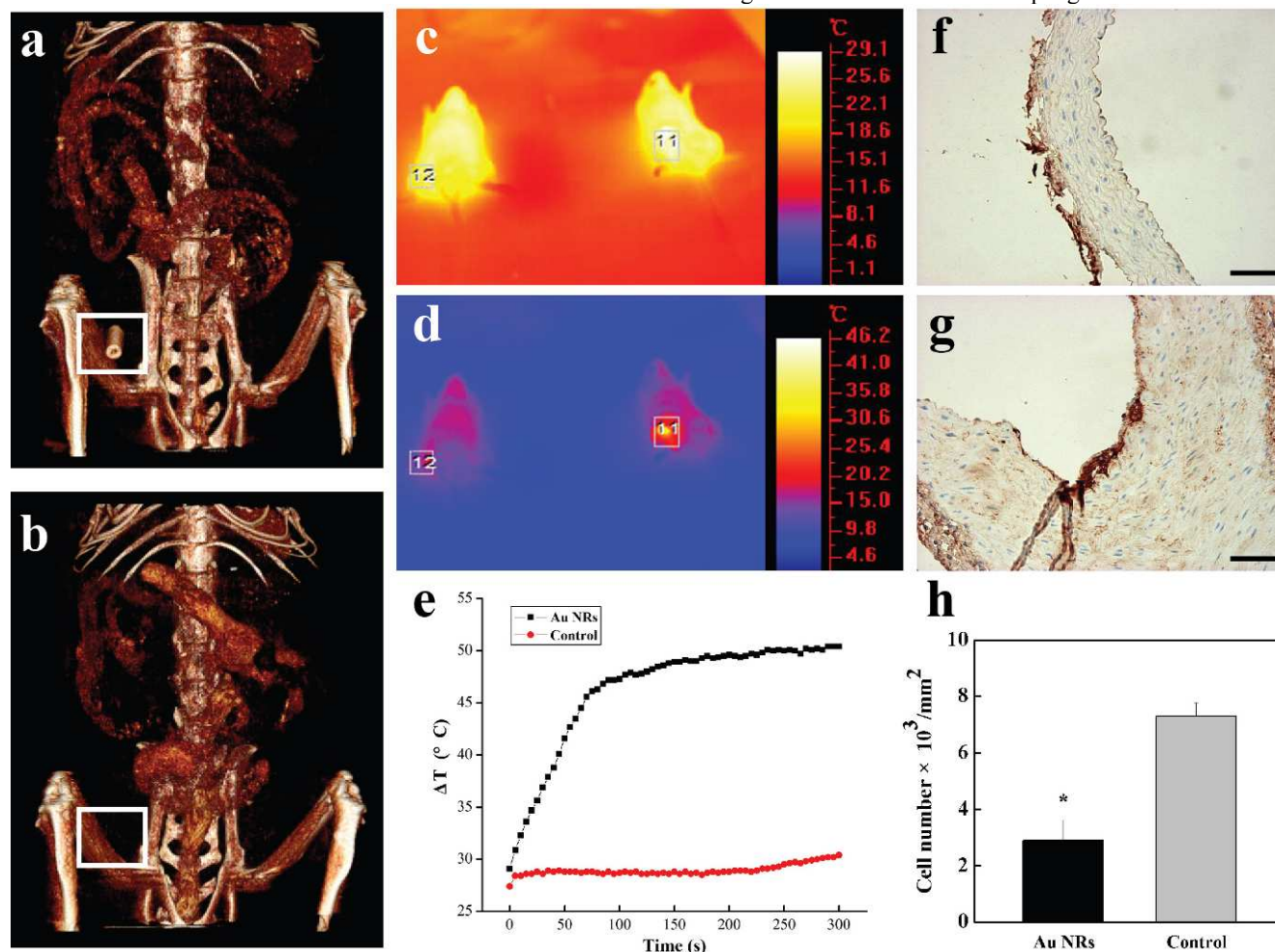


Fig. 6 *In vivo* PTT of femoral artery restenosis with the Au NRs. *In vivo* 3D micro-CT images of the femoral artery before (b) and after (a) the intravenous injection of the Au NRs. IR thermal images (c, d) of Apo E mice injected with the Au NRs (the right mouse, indicated region 11) or saline (the left mouse, indicated region 12) via the intravenous injection, respectively, irradiated with the 808 nm laser (2 W/cm^2) at a time point of 0 (c) and 300 s (d). (e) The temperature profiles in regions 11 and 12 as a function of the irradiation time. (f, g) The representative histological examination sections stained with CD68, of the corresponding *ex vivo* the femoral artery restenosis regions, after irradiation for 10 min. The irradiation source is an 808 nm laser with the safe power density of 2 W/cm^2 . (h) Statistical analysis of the macrophages number between Au NRs with and without PTT. Scale bars in f and g: 100 μm .

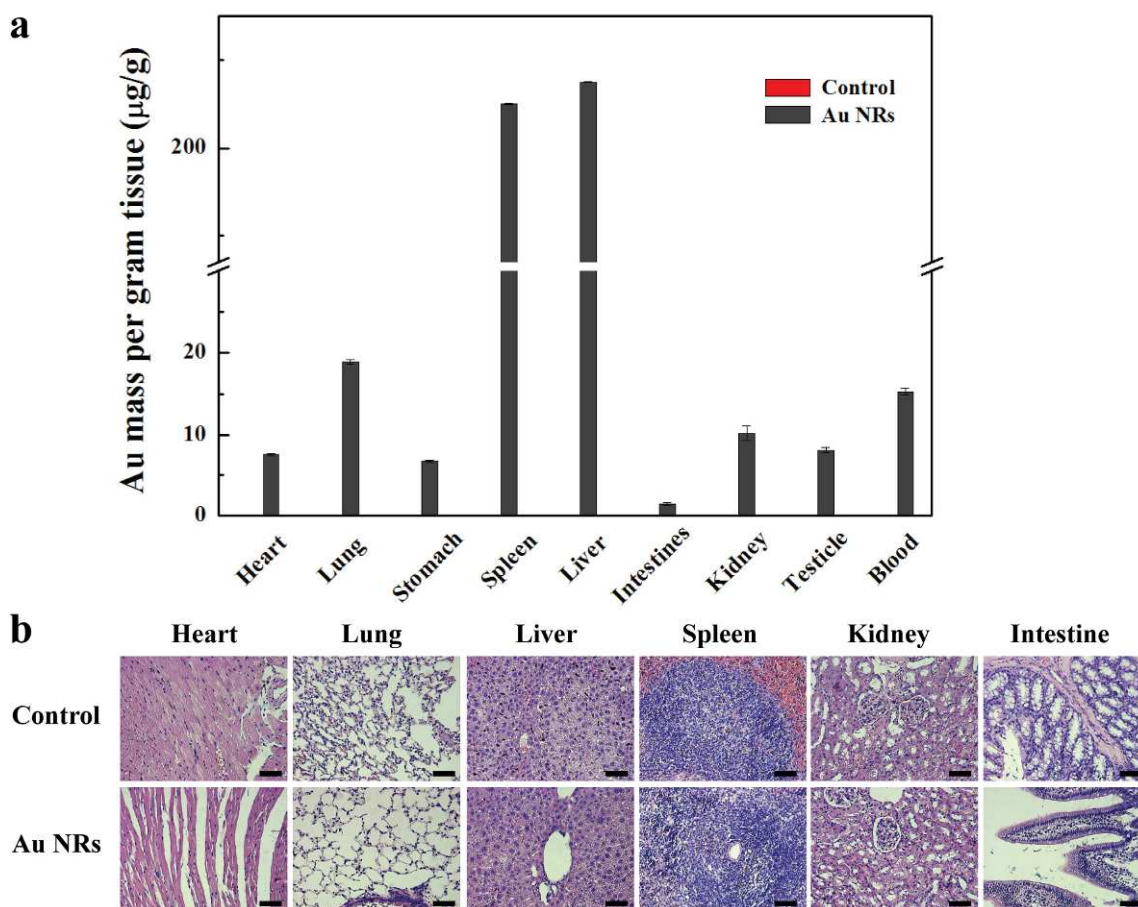


Fig. 7 Bio-distribution and histochemical staining of the Au NRs. (a) ICP analysis of the bio-distribution of the Au NRs in the major organs (heart, lung, stomach, spleen, liver, intestines, kidney, testicle, and blood) after the PTT. (b) Representative images of HE staining of the main visceral organs in the Apo E mice treated with the Au NRs after the PTT. All of the organs appear histologically normal. Scale bars: 100 μm . All scale bars = 100 μm .

We resected and then dissected the major organs (i.e., the heart, lung, liver, spleen, kidney, and intestines) for histological analysis after the PTT, all of which showed certain particle accumulation, as shown by ICP-AES. Sections of major organs were stained with H&E (Fig. 7b), compared with the control groups, no significant organ damage and inflammatory lesions were found in the mice injected with the Au NRs, which suggests the excellent biocompatibility of the Au NRs to the major organs.

Recently, localized PTT has been investigated for targeted cell ablation, given that the sudden generation of heat can promote denaturation and disruption of intracellularly organized biomolecules.⁴⁰ To overcome nonspecific organ uptake and cytotoxicity, targeted Au NRs, modified with specific protein markers or molecules are urgently needed. The key objective of photothermal ablation is to damage the targeted regions without destroying the surrounding normal tissues.⁴¹ Our results demonstrated that the Au NRs used in the PTT exhibit good biocompatibility, high photothermal conversion efficiency, and excellent PTT in the NIR region.

4. Conclusions

In summary, we have developed a facile method to synthesize nontoxic and good biocompatible Au NRs for efficient imaging and photothermal ablation of macrophages *in vitro* and *in vivo*. The combined *in vitro* results of CCK8 assay, calcein AM/PI

staining, flow cytometry analysis, TEM, CT imaging, and photothermal ablation treatment show that the Au NRs are non-cytotoxic at the given concentration and are able to image and ablate macrophages, even with lower NIR powers. In addition, the *in vivo* therapeutic experiments demonstrated that the Au NRs could image and PTT of inflammatory macrophages in the femoral artery restenosis of Apo E mice. Findings from our results suggest that the Au NRs have a great potential to be used as multifunctional theranostic agents for imaging and photothermal therapy of inflammatory macrophages, which paves the way for further theranostics of atherosclerosis and other inflammatory diseases.

Acknowledgements

This research is financially supported by the National Natural Science Foundation of China (81370423), the Natural Science Foundation of Shanghai Science and Technology Committee (Grant No. 134119a2100, 15YF1406900 and 20124Y132), and Doctoral Innovation Fund Projects from Shanghai JiaoTong University School of Medicine (BXJ201428).

The authors report no conflicts of interest in this work.

Notes and references

ARTICLE

1. C. Weber and H. Noels, *Nature medicine*, 2011, 17, 1410-1422.
2. P. Libby, P. M. Ridker and G. K. Hansson, *Nature*, 2011, 473, 317-325.
3. S. Allahverdian, A. C. Chehroudi, B. M. McManus, T. Abraham and G. A. Francis, *Circulation*, 2014, 129, 1551-1559.
4. M. Nurunnabi, Z. Khatun, G. R. Reeck, D. Y. Lee and Y. K. Lee, *ACS applied materials & interfaces*, 2014, 6, 12413-12421.
5. **X. Song, C. Liang, H. Gong, Q. Chen, C. Wang and Z. Liu, *Small*, 2015, DOI: 10.1002/sml.201500550.**
6. **B. Cirera, Y. Q. Zhang, J. Bjork, S. Klvatskaya, Z. Chen, M. Ruben, J. V. Barth and F. Klappenberger, *Nano letters*, 2014, 14, 1891-1897.**
7. **J. Li, J. Han, T. Xu, C. Guo, X. Bu, H. Zhang, L. Wang, H. Sun and B. Yang, *Langmuir : the ACS journal of surfaces and colloids*, 2013, 29, 7102-7110.**
8. C. L. Chen, L. R. Kuo, S. Y. Lee, Y. K. Hwu, S. W. Chou, C. C. Chen, F. H. Chang, K. H. Lin, D. H. Tsai and Y. Y. Chen, *Biomaterials*, 2013, 34, 1128-1134.
9. H. H. Joo, H. J. Jo, T. D. Jung, M. S. Ahn, K. B. Bae, K. H. Hong, J. Kim, J. T. Kim, S. H. Kim and Y. I. Yang, *International journal of colorectal disease*, 2012, 27, 1437-1443.
10. J. W. Xiao, S. X. Fan, F. Wang, L. D. Sun, X. Y. Zheng and C. H. Yan, *Nanoscale*, 2014, 6, 4345-4351.
11. T. Mironava, M. Hadjiargyrou, M. Simon and M. H. Rafailovich, *Nanotoxicology*, 2014, 8, 189-201.
12. M. F. Tsai, S. H. Chang, F. Y. Cheng, V. Shanmugam, Y. S. Cheng, C. H. Su and C. S. Yeh, *ACS nano*, 2013, 7, 5330-5342.
13. V. Amirbekian, M. J. Lipinski, K. C. Briley-Saebo, S. Amirbekian, J. G. Aguinaldo, D. B. Weinreb, E. Vucic, J. C. Frias, F. Hyafil, V. Mani, E. A. Fisher and Z. A. Fayad, *Proceedings of the National Academy of Sciences of the United States of America*, 2007, 104, 961-966.
14. C. Psarros, R. Lee, M. Margaritis and C. Antoniadis, *Nanomedicine : nanotechnology, biology, and medicine*, 2012, 8 Suppl 1, S59-68.
15. J. Vonnemann, N. Beziere, C. Bottcher, S. B. Riese, C. Kuehne, J. Dervede, K. Licha, C. von Schacky, Y. Kosanke, M. Kimm, R. Meier, V. Ntziachristos and R. Haag, *Theranostics*, 2014, 4, 629-641.
16. J. Yong, K. Needham, W. G. Brown, B. A. Nayagam, S. L. McArthur, A. Yu and P. R. Stoddart, *Advanced healthcare materials*, 2014, DOI: 10.1002/adhm.201400027.
17. C. Leduc, S. Si, J. Gautier, M. Soto-Ribeiro, B. Wehrle-Haller, A. Gautreau, G. Giannone, L. Cognet and B. Lounis, *Nano letters*, 2013, 13, 1489-1494.
18. B. Li, Q. Wang, R. Zou, X. Liu, K. Xu, W. Li and J. Hu, *Nanoscale*, 2014, 6, 3274-3282.
19. K. Hayashi, M. Nakamura and K. Ishimura, *Advanced healthcare materials*, 2013, 2, 756-763.
20. J. Qin, K. Li, C. Peng, X. Li, J. Lin, K. Ye, X. Yang, Q. Xie, Z. Shen, Y. Jin, M. Jiang, G. Zhang and X. Lu, *Biomaterials*, 2013, 34, 4914-4925.
21. J. B. Qin, K. A. Li, X. X. Li, Q. S. Xie, J. Y. Lin, K. C. Ye, M. E. Jiang, G. X. Zhang and X. W. Lu, *International journal of nanomedicine*, 2012, 7, 5191-5203.
22. X. Liu, B. Li, F. Fu, K. Xu, R. Zou, Q. Wang, B. Zhang, Z. Chen and J. Hu, *Dalton transactions*, 2014, 43, 11709-11715.
23. N. M. Pires, D. Eefting, M. R. de Vries, P. H. Quax and J. W. Jukema, *Heart*, 2007, 93, 922-927.
24. R. Choi, J. Yang, J. Choi, E. K. Lim, E. Kim, J. S. Suh, Y. M. Huh and S. Haam, *Langmuir : the ACS journal of surfaces and colloids*, 2010, 26, 17520-17527.
25. **R. Bhattacharya and P. Mukherjee, *Advanced drug delivery reviews*, 2008, 60, 1289-1306.**
26. **K. L. Aillon, Y. Xie, N. El-Gendy, C. J. Berkland and M. L. Forrest, *Advanced drug delivery reviews*, 2009, 61, 457-466.**
27. **B. Fadeel and A. E. Garcia-Bennett, *Advanced drug delivery reviews*, 2010, 62, 362-374.**
28. **F. Osaki, T. Kanamori, S. Sando, T. Sera and Y. Aoyama, *Journal of the American Chemical Society*, 2004, 126, 6520-6521.**
29. **W. H. De Jong, W. I. Hagens, P. Krystek, M. C. Burger, A. J. Sips and R. E. Geertsma, *Biomaterials*, 2008, 29, 1912-1919.**
30. D. Wang, Z. Xu, H. Yu, X. Chen, B. Feng, Z. Cui, B. Lin, Q. Yin, Z. Zhang, C. Chen, J. Wang, W. Zhang and Y. Li, *Biomaterials*, 2014, 35, 8374-8384.
31. Z. Chen, Q. Wang, H. Wang, L. Zhang, G. Song, L. Song, J. Hu, H. Wang, J. Liu, M. Zhu and D. Zhao, *Advanced materials*, 2013, 25, 2095-2100.
32. V. Shanmugam, S. Selvakumar and C. S. Yeh, *Chemical Society reviews*, 2014, DOI: 10.1039/c4cs00011k.
33. **Y. Sheng, M. Lin, X. Li, H. Hao, X. Lin, H. Sun and H. Zhang, *Part. Part. Syst. Charact.* 2014, 31, 788-793.**

34. S. N. Goldberg, G. S. Gazelle and P. R. Mueller, *AJR. American journal of roentgenology*, 2000, 174, 323-331.
35. L. Meng, L. Niu, L. Li, Q. Lu, Z. Fei and P. J. Dyson, *Chemistry*, 2012, 18, 13314-13319.
36. Z. Zhou, Y. Sun, J. Shen, J. Wei, C. Yu, B. Kong, W. Liu, H. Yang, S. Yang and W. Wang, *Biomaterials*, 2014, 35, 7470-7478.
37. B. Jang, S. Park, S. H. Kang, J. K. Kim, S. K. Kim, I. H. Kim and Y. Choi, *Quantitative imaging in medicine and surgery*, 2012, 2, 1-11.
38. **Y. Akiyama, T. Mori, Y. Katayama and T. Niidome**, *Journal of controlled release : official journal of the Controlled Release Society*, 2009, 139, 81-84.
39. **J. Qin, C. Peng, B. Zhao, K. Ye, F. Yuan, Z. Peng, X. Yang, L. Huang, M. Jiang, Q. Zhao, G. Tang and X. Lu**, *International journal of nanomedicine*, 2014, 9, 5575-5590.
40. G. Song, J. Shen, F. Jiang, R. Hu, W. Li, L. An, R. Zou, Z. Chen, Z. Qin and J. Hu, *ACS applied materials & interfaces*, 2014, 6, 3915-3922.
41. H. Kosuge, S. P. Sherlock, T. Kitagawa, R. Dash, J. T. Robinson, H. Dai and M. V. McConnell, *Journal of the American Heart Association*, 2012, 1, e002568.